COMBUSTION CHARACTERISTICS OF METHANOL WITH TURBULENT JET IGNITION IN A CONSTANT VOLUME COMBUSTION CHAMBER

Yi Wang[1], Chengyun Li[2], Maohui Su[3,5], Wenhua Zhou[1], Francis Oppong[4], Cangsu Xu[1,5*]

[1]College of Energy Engineering, State Key Laboratory of Clean Energy Utilization, Zhejiang University, Hangzhou, 310027, China P.R.

[2]Ningbo Geely Royal Engine Components Co. Ltd., Ningbo, China, 315336

[3]Zhejiang Geely Farizon New Energy Commercial Vehicle Group Co. Ltd., Hangzhou, 310051, China P.R.

[4]College of Mechanical and Electrical Engineering, China Jiliang University, Hangzhou, 310018, China P.R.

[5]School of New Energy and Intelligent Networked Automobile, University of Sanya, Sanya, 572022, China P.R.

[*]Corresponding author: xucangsu@zju.edu.cn

Methanol is a renewable and sustainable energy source with potential to overcome energy scarcity, global warming, and environmental pollution caused by the overdependence on fossil energy. However, its application in engines faces challenges, particularly the cold start issues. Turbulent Jet Ignition (TJI) presents a promising solution due to its advantage of multipoint ignition, and thereby a comprehensive study of TJI can contribute to guide the design and optimization of methanol engines. This work establishes an experimental system, employing the high-speed schlieren imaging technique to observe the propagation of methanol jet flames, and investigates the influence on the combustion characteristics of various operating parameters, such as the initial temperature and pressure and the intervals between the two ignitions. The results indicate that the propagation of the jet flame accelerates with the equivalence ratio increasing from 0.8 to 1.2. When the equivalence ratio is 1.0 and 1.2, the higher initial pressure results in slower development of the jet flame. Additionally, a short ignition interval leads to sluggish jet flame development and prolonged combustion duration, while an excessively prolonged ignition interval makes it impossible to generate effective jet flame. This research provides valuable insights for optimizing the jet ignition operation and enhancing the efficiency of methanol engines.

Keywords: *Methanol; Jet ignition; Contour recognition; Constant volume bomb; Combustion characteristics; Flame form*

1. Introduction

The excessive reliance on fossil energy has led to increasingly severe issues, including energy scarcity, global warming and environmental pollution [1]. As a renewable and sustainable fuel, methanol offers a promising solution to these challenges. Methanol has higher synthetic efficiency than ethanol and synthetic hydrocarbons [2] and superior thermal efficiency in combustion systems [3], meaning a dual advantage in enhancing primary energy utilization. Furthermore, methanol has high resistance to detonation [4], which allows the use of higher compression ratios and more optimal ignition timing under full engine operating conditions, thus increasing the thermal efficiency and power of engines [5]. Also, methanol has a lower stoichiometric air-fuel ratio than gasoline, leading to a higher proportion of triatomic molecules (CO_2 and H_2O) in its combustion products [6].

However, the cold start issue is a major challenge to methanol engines, which is usually caused by methanol's lower stoichiometric air-fuel ratio, increased evaporation and risk of short-circuiting between spark plug electrodes due to its electrical conductivity when the spray is poorly atomized [3, 7]. In this context, investigating the spray atomization of methanol is crucial for enhancing the performance of methanol engines. Consequently, numerous studies on methanol spray characteristics have been conducted in recent years, as summarized in Tab. 1.

Table 1 Pertinent studies on methanol spray characteristics

No.	Methods	Parameters	Characteristics/ Objectives	Refs.
1	High-speed shadowing imaging	Ambient density (1.2-100 kg/m³); Injection pressure (55-100 MPa)	Sauter Mean Diameter; Penetration distance; Spray angle	[8]
2	High-speed photography	Injection pressure (80 MPa);	Cycle-to-cycle variation quantification; Evaporative cooling-spray interaction	[9]
3	High-speed photography; Phase doppler particle analyzer	Ambient pressure (0.01-0.1 MPa); Fuel temperature (298-393 k)	Flash-boiling spray collapse mechanisms; Droplet velocity profiles; Fuel property effects	[10]
4	Planar Laser-Induced Fluorescence; Mie scattering	Ambient pressure (0.04, 0.1 MPa); Fuel temperature (298, 328, 363 k)	Phase-separated spray morphology; Cold-start spray optimization	[11]
5	Phase doppler particle analyzer	Injection pressure (0.3-0.5 MPa)	Cavitation region expansion in nozzle; Discharge coefficient vs. temperature; Sauter Mean Diameter	[12]
6	Laser diffraction technology	Ambient temperature (298-323 K); Injection pressure (1.3-2.1 MPa)	Dominant effect of ambient temperature on droplet size; Atomization characteristics	[13]

Turbulent Jet Ignition (TJI) is an efficient strategy to optimize engine performance and address the cold-start issue, proposed and developed by Li Gang [14] and Gussak [15], respectively. TJI offers the advantage of multipoint ignition, as reactive free radicals in combustion products from precombustion chamber can ignite mixtures in the main chamber at multiple dispersed points. As summarized in Tab. 2, many researchers have explored the potential of TJI technology in improving power and emission performance of engines. However, current literatures mainly focus on the conventional fuels and alternative fuels such as hydrogen, while the research on TJI with methanol remains relatively limited. Considering the significant advantages of multipoint ignition enabled by TJI, a comprehensive study of TJI with methanol could provide valuable insights for the design and optimization of methanol engines.

Table 2 Summary of Relevant Studies on TJI

No.	Methods	Fuels	Objectives	Refs.
1	Jet Controlled Compression Ignition	Diesel	Improving pre-mix combustion rate in diesel engines	[16, 17]
2	Planar Laser-Induced Fluorescence; OH* chemiluminescence imaging	Methane	Investigating the effects of precombustion chamber volume and orifice diameter on precombustion chamber jet and main combustion chamber ignition	[18, 19]
3	High-speed visible intensified imaging; Low-speed infrared imaging	Natural gas	Investigating the effect of fuel spark position, equivalence ratio, orifice size, and geometry on ignition patterns in the main combustion chamber	[20]
4	Self-designed air-assisted pre-chamber apparatus	Hydrogen; Gasoline; Methane		[21–23]

In this research, the combustion characteristics of TJI with methanol are investigated, and the influence of various condition parameters are comprehensively compared and discussed.

2. Experimental Setup

2.1. Experimental equipment

The diagram of the experimental apparatus is given in Fig. 1, which mainly consists of a constant volume combustion facility, a high-speed schlieren system and an electronically controlled ignition system.

The constant volume combustion facility consists of a main chamber and a precombustion chamber. The internal volume of the main combustion chamber is 1.6 L with two quartz windows on opposite sides, each with a diameter of 90 mm. The precombustion chamber has a volume of 0.01 L, with a jet orifice of 3 mm. Moreover, a pressure sensor (Kistler 6115B)[24] and a temperature thermocouple are installed to detect combustion pressure (p) and initial temperature in the main chamber, respectively. The estimated response time of Kistler 6115B is less than 20 μs based on its acoustic natural frequency of 65 kHz, thereby enabling precise capture of rapid pressure transients. Additionally, the main chamber is heated by uniformly distributed heating rods in walls.

The propagation of jet flames in the main chamber is captured by the high-speed schlieren, which consists of an optical source, a high-speed camera and two schlieren mirrors. The high-speed camera has an image size of 1024×1024 pixels, a frame rate of 12800 FPS, and a maximum shutter speed of 1/2000 s.

The ignition system is primarily comprised of two spark plugs and an electronic control unit (ECU). The first spark plug ignites the mixture in the main combustion chamber, building up the pressure field, while the second spark plug ignites the mixture in the precombustion chamber to generate a reactive jet.

2.2. Experimental conditions

In the study, the impacts of initial conditions on combustion characteristics are investigated by varying initial pressure (P_0 = 0.1, 0.2 and 0.3 MPa) and equivalence ratio (φ = 0.8, 1.0 and 1.2) of the methanol-air mixtures in the main combustion chamber with the initial temperature (T_0) of 373 K. P_0 and φ are regulated using pressure gauge and mass flow controllers for the inlet gas, alongside injecting corresponding amount of methanol. Additionally, the effects of the ignition interval between two sparks (2, 3 and 4 ms), which is controlled by the ECU, are examined with the T_0 = 403 K. Experiments are conducted three times under each condition, and the average value is taken to minimize random errors.

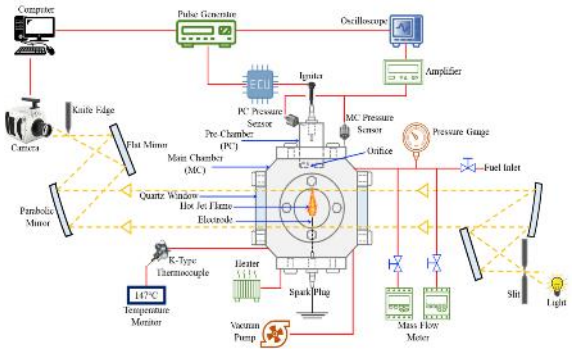

Fig. 1 Schematic of the Experimental Apparatus

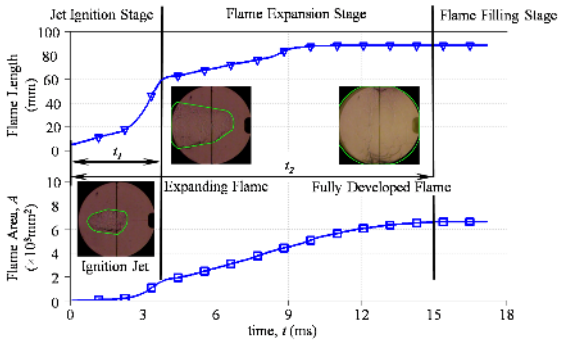

Fig. 2 Development stage of a jet flame

3. Data Analysis Methods

3.1. Image processing and analysis method

The image processing program is implemented using Python with OpenCV, employing a differential method to extract the flame profile, which can be found in previous studies [25]. Considering that the flame velocity of a turbulent flame is difficult to directly measure due to its irregular flame fronts, the average area growth rate of the flame, $(dA/dt)_{avg}$, is introduced to evaluate the flame propagation.

According to the location and shape of the jet flame, the process of flame development is divided into three stages: the jet ignition stage, the flame expansion stage, and the flame filling stage, as shown in Fig. 2. The jet ignition stage is defined as the period from the ignition in the main combustion chamber to the first instance (t_1) when the flame reaches the boundary of the window. The jet, ejected from the precombustion chamber, carries high-temperature combustion products and active radicals, facilitating the multipoint ignition of the methanol-air mixtures in the main chamber. In the subsequent flame

expansion stage, the turbulent flame expands and its surface develops radially. The flame filling stage refers to the period after the first instance (t_2) when the flame completely fills the window area, indicating that the flame has propagated beyond the capture area.

3.2. Pressure analysis method

When the flame expands beyond the window area, pressure analysis is employed to further study the combustion characteristics.

The spherical volume corresponding to the diameter of the window represents 22% of the internal volume of the main combustion chamber. Under the ideal assumption, when the flame profile completely fills the window, the volume of the unburned mixture will be approximately compressed to 78% of the initial state. Simultaneously, the pressure in the main chamber will increase to 1.28 times its initial value. In practice, the pressure at the edge of the unburned mixture is 1.3 to 1.4 times P_0, as a result of the heating effect of combustion and compression. Consequently, the pressure analysis is conducted after the pressure in the main chamber (p) reached 1.4 times P_0, at the time denoted as t_v. Moreover, the combustion time, t_c is defined as the moment when p reaches its maximum value, as annotated in Fig. 3.

The value of the maximum pressure rise rate, $(dp/dt)_{max}$, is affected by the volume of the constant combustion chamber. To account for this volume effect, the deflagration index K_G is used, which helps assess the intensity of the combustion process and the safety of combustibles. K_G is calculated using Eq. (1), which removes the volume effect. A higher K_G indicates a more intense combustion, higher likelihood of explosion, and more severe consequences of the explosion.

$$K_G=(\frac{dp}{dt})_{max}V^{1/3} \tag{1}$$

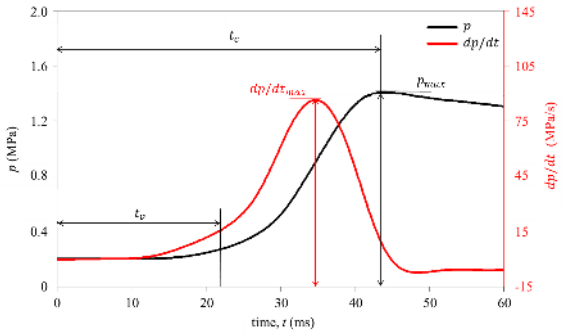

Fig. 3 Evolution of pressure and pressure rise rate during a jet ignition experiment

4. Results and Discussion

4.1. Effect of the equivalence ratio

As presented in Tab. 3, both t_2 and t_c decrease with φ increasing from 0.8 to 1.2, while $(dA/dt)_{avg}$, P_{max} and $(dp/dt)_{max}$ increase, suggesting that the increasing φ enhances the expansion rate of the jet flame, as further demonstrated in **Error! Reference source not found.**-6(a). In lean combustion, the lower fuel content in the main combustion chamber reduces the reaction intensity, leading to a slower development of the jet flame. Conversely, oxidization reactions between oxygen and fuel molecules

become more intense under rich combustion conditions, releasing more energy and active radicals, which promotes the expansion of the jet flame.

Table 3 Combustion characteristics of jet flames with various φ (T_0 = 373 K)

P_0 (MPa)	φ	$(dA/dt)_{avg}$ (mm^2/ms)	t_1 (ms)	t_2 (ms)	t_c (ms)	P_{max} (MPa)	K_G (MPa*m/s)	$(dp/dt)_{max}$ (MPa/s)
0.1	0.8	277.7	7.0	22.2	63.2	0.5	1.3	11.0
	1.0	386.3	3.9	14.7	37.5	0.6	3.0	25.3
	1.2	406.4	5.2	12.7	30.4	0.7	4.4	36.8
0.2	0.8	121.3	40.8	54.8	87.1	1.2	4.9	41.0
	1.0	267.5	6.4	20.1	51.1	1.3	4.9	41.4
	1.2	302.6	10.9	18.1	37.1	1.4	10.3	86.5
0.3	0.8	155.0	6.9	39.3	126.6	1.5	2.9	24.8
	1.0	208.8	10.9	31.8	59.8	1.9	7.1	60.1
	1.2	301.1	12.7	22.0	43.8	2.1	13.9	116.9

At P_0 of 0.1 and 0.2 MPa, t_1 reaches its minimum value at φ = 1.0, confirming the fastest flame propagation under the stoichiometric conditions. However, t_1 shows a monotonic increase with the increasing φ at P_0 of 0.3 MPa, and **Error! Reference source not found.**-6(b) provides an insight of this trend. As φ increases, the spherical flame generated by the center electrode expands more rapidly, while the initial jet flame energy is insufficient to impact the development of the spherical flame. Moreover, as the intensity of the jet increases, the jet and spherical flames merge only after 10.0 ms following ignition.

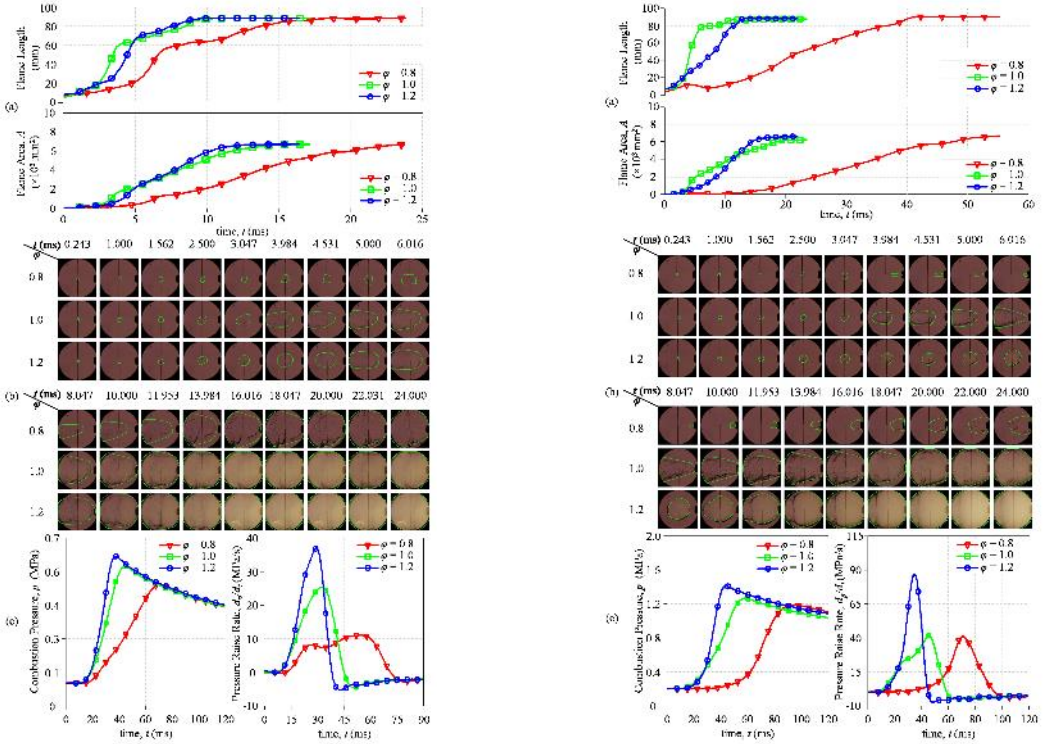

Fig. 4 Evolution of (a) flame size; (b) flame profile; and (c) combustion pressure during the propagation of the jet flame (T_0 = 373 K and P_0 = 0.1 MPa)

Fig. 5 Evolution of (a) flame size; (b) flame profile; and (c) combustion pressure during the propagation of the jet flame (T_0 = 373 K and P_0 = 0.2 MPa)

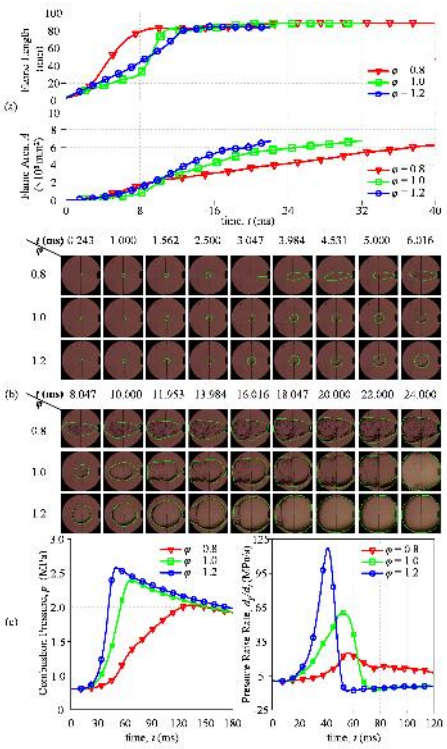

Fig. 6 Evolution of (a) flame size; (b) flame profile; and (c) combustion pressure during the propagation of the jet flame (T_0 = 373 K and P_0 = 0.3 MPa)

It is noteworthy that when φ is 0.8 and p is 0.2 MPa, the developing spherical flame is blown out by the jet injected from the precombustion chamber, as depicted in in Fig 5(b). Subsequently, the jet flame continues to propagate, indicating that the stability of the jet flame surpasses that of the conventional flame.

4.2. Effect of the initial pressure

Tab. 3 presents the combustion characteristics of jet flames with various P_0, showing that P_{max} increases while t_c decreases with P_0 elevated from 0.1 to 0.3 MPa. This trend is attributed to the higher P_0, which increases the molecular density and quantity in the main combustion chamber, thereby enhancing energy release and prolonging the reaction duration. The trends of other combustion characteristics remain consistent as P_0 increases at φ of 1.0 and 1.2, but deviate at φ of 0.8. As illustrated in Fig. 7-9(b), the jet extinguishes the developing spherical flame at P_0 of 0.2 and 0.3 MPa, resulting in the observed deviation at φ of 0.8. The extinguishment occurs because the jet velocity exceeds the laminar flame velocity, thereby disrupting the formation and stabilization of the spherical flame.

When φ = 1.0 and 1.2, $(dA/dt)_{avg}$ decreases as P_0 increases from 0.1 to 0.3 MPa, while t_1 and t_2 increase, indicating that the propagation of jet flames, similar to that of laminar flames [26], slows down

with rising initial pressure increasing. Under the same combustion process, the energy release intensifies with elevating P_0, resulting in higher heat release and consequently higher $(dp/dt)_{max}$ and K_G.

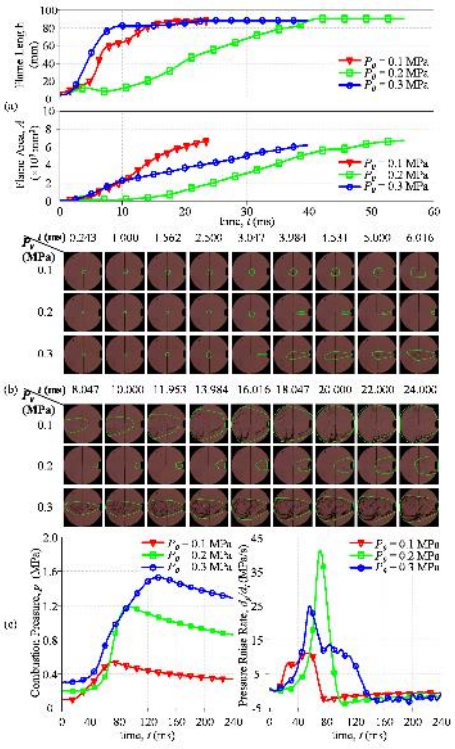

Fig. 7 Evolution of (a) flame size; (b) flame profile; and (c) combustion pressure during the propagation of the jet flame (T_0 = 373 K and φ = 0.8)

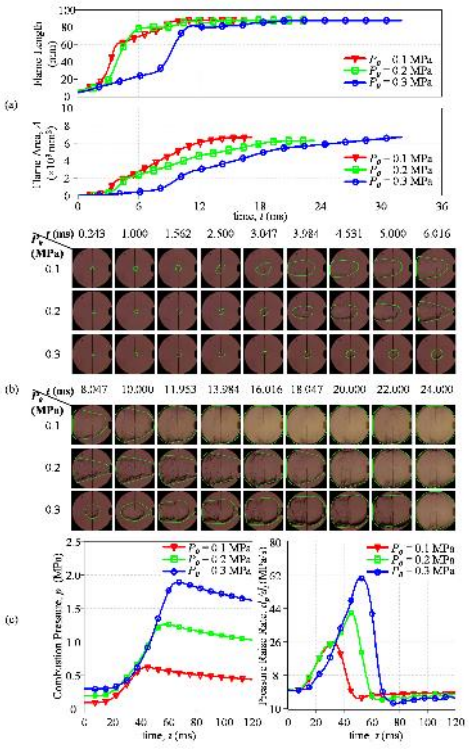

Fig. 8 Evolution of (a) flame size; (b) flame profile; and (c) combustion pressure during the propagation of the jet flame (T_0 = 373 K and φ = 1.0)

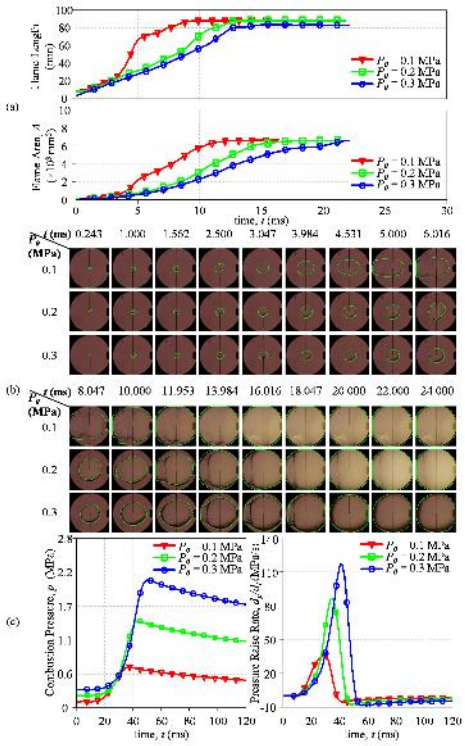

Fig. 9 Evolution of (a) flame size; (b) flame profile; and (c) combustion pressure during the propagation of the jet flame (T_0 = 373 K and φ = 1.2)

4.3. Effect of the Ignition Interval

The time intervals between the ignition of the sparks in the main combustion chamber and precombustion chamber are set as 2, 3 and 4 ms, and the corresponding experimental results are shown in Tab. 4 and Fig. 10-12. As the interval increased from 2 to 3 ms, the flame propagation accelerates, as evidenced by the trends of $(dA/dt)_{avg}$, t_1 and t_2. However, the opposite trend is observed with the interval increasing from 3 to 4 ms. Specifically, the jet flame is more intense at an interval of 3 ms than that of 2 ms as shown in Fig. 12, indicating that a longer interval benefits more sufficient flame propagation. Conversely, at an interval of 4 ms, the spherical flame propagates radially without the formation of a distinct jet flame, leading to a slower flame propagation compared to the 3 ms interval.

Table 4 Combustion characteristics of jet flames with various ignition intervals (T_0 = 403 K, P_0 = 0.1 MPa and φ = 0.8)

Ignition Interval (ms)	$(dA/dt)_{avg}$ (mm^2/ms)	t_1 (ms)	t_2 (ms)	t_c (ms)	P_{max} (MPa)	K_G (MPa*m/s)	$(dp/dt)_{max}$ (MPa/s)
2	203.3	7.2	23.3	58.2	0.5	1.8	15.0
3	389.4	4.1	15.0	38.0	0.6	2.5	21.3
4	363.7	14.4	17.0	37.6	0.6	4.2	35.5

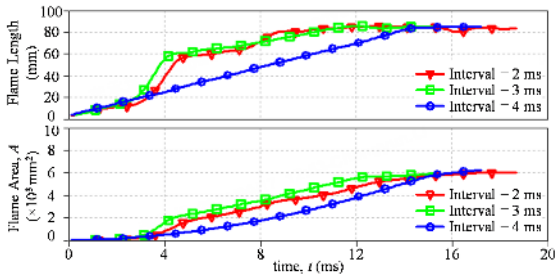

Fig. 10 Evolution of jet flame characteristics under varied ignition intervals (T_0 = 403 K, P_0 = 0.1 MPa and φ = 0.8)

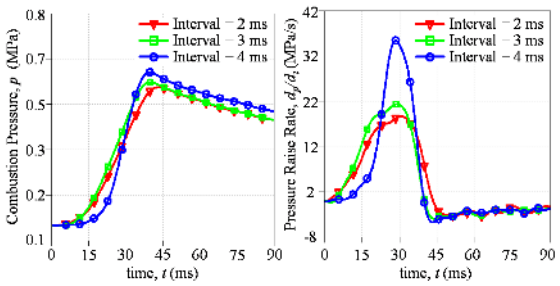

Fig. 11 Evolution of combustion pressure under varied ignition intervals (T_0 = 403 K, P_0 = 0.1 MPa and φ = 0.8)

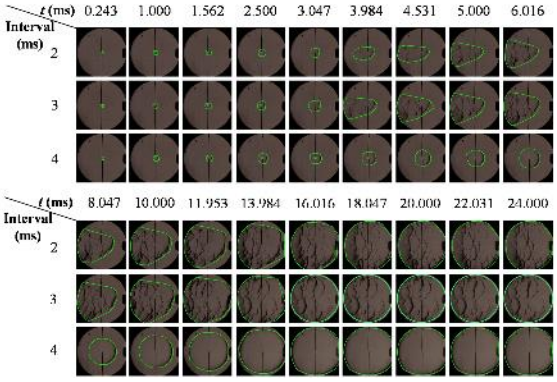

Fig. 12 Propagation of jet flames under varied ignition intervals (T_0 = 403 K, P_0 = 0.1 MPa and φ = 0.8)

It is observed that K_G and $(dp/dt)_{max}$ increase, while t_c decreases with the increase of the ignition interval. At intervals of 2 and 3 ms, the mixture is ignited at multiple dispersed points by the jet, avoiding pressure concentration and resulting in smaller K_G and $(dp/dt)_{max}$ than that at the intervals of 4 ms, in which the flame is center-ignited. Furthermore, the more moderate turbulence at an interval of 2 ms leads to a longer combustion period, causing K_G and $(dp/dt)_{max}$ to be smaller than those observed at the 3 ms interval.

5. Conclusion

In this study, an electrically controlled experiment setup is designed to investigate the combustion characteristics of TJI, using high-speed schlieren imaging technology. The effects of initial conditions and electronic control strategies on TJI combustion characteristics are analyzed. The main conclusions of this research as follows:

1. As φ increases from 0.8 to 1.2, the expansion of the jet flame accelerates due to intensified oxidation reactions, whereas it is suppressed at lean combustion conditions. At P_0 of 0.1 and 0.2 MPa, the shortest t_1 is observed at φ = 1, indicating the most rapid flame propagation. However, at P_0 = 0.3 MPa, t_1 increases with φ as the spherical flame expands more rapidly. Notably, at φ = 0.8 and P_0 = 0.2 MPa, the jet flame remains stable even after the spherical flame extinguished, demonstrating its superior stability.

2. The combustion process remains consistent at φ = 1.0 and 1.2 but deviates at φ = 0.8, where the jet extinguishes the developing spherical flame at P_0 = 0.2 and 0.3 MPa due to excessive jet velocity. For φ = 1.0 and 1.2, $(dA/dt)_{avg}$ decreases while t_1 and t_2 increase with rising P_0, indicating a deceleration in jet flame propagation. As P_0 increases from 0.1 to 0.3 MPa, P_{max}, $(dp/dt)_{max}$ and K_G rise while t_c decreases due to higher molecular density intensifying chemical reaction and prolonging energy release duration.

3. The speed of flame propagation peaks at a 3 ms ignition interval, with a stronger jet flame enhancing efficiency, while the absence of a distinct jet slows propagation at an interval of 4 ms. K_G and $(dp/dt)_{max}$ increase while t_c decreases with longer intervals. Multi-point ignition with intervals of 2 and 3 ms disperses pressure, reducing K_G and $(dp/dt)_{max}$, compared the center ignition with the interval of 4 ms.

Data Availability

Some or all data, models, or code that support the findings of this study are available from the corresponding author upon reasonable request.

Acknowledgements

The authors are indebted to the Ningbo Major Science and Technology Project (20212ZDYF020041) for funding this work.

Nomenclature

The following terms are used in this paper:

A: flame area;

K_G: deflagration index;

p: pressure in the main combustion chamber;

P_{max}: the maximum pressure;

P_0: the initial pressure in the main combustion chamber;

$(dA/dt)_{avg}$: the average flame area growth rate;

dp/dt: pressure rise rate;

t: the time elapsed since the ignition of the spark plug in the main combustion chamber;

t_c: the moment when the pressure reaches its maximum value;

t_v.: the moment when the pressure reaches 1.4 times P_0;

T_0: the initial temperature in the main combustion chamber;

t_1: the first instance when the flame reaches the boundary of the window;

t_2: the first instance when the flame completely fills the window area; and

φ: the equivalence ratio of methanol and air in the main combustion chamber.

Reference

[1]Mukherji, A., et al., SYNTHESIS REPORT OF THE IPCC SIXTH ASSESSMENT REPORT (AR6)

[2]Verhelst, S., et al., Methanol As A Fuel For Internal Combustion Engines, *Progress in Energy and Combustion Science, 70* (2019), pp. 43-88

[3]Çelebi, Y., Aydın, H., An Overview On The Light Alcohol Fuels In Diesel Engines, *Fuel, 236* (2019), pp. 890-911

[4]Turner, J.W.G., et al., Alcohol Fuels For Spark-Ignition Engines: Performance, Efficiency And Emission Effects At Mid To High Blend Rates For Binary Mixtures And Pure Components, *Proceedings of the Institution of Mechanical Engineers, Part D: Journal of Automobile Engineering, 232* (2018), 1, pp. 36-56

[5]Huang, Q., et al., On The Use Of Artificial Neural Networks To Model The Performance And Emissions Of A Heavy-Duty Natural Gas Spark Ignition Engine, *International Journal of Engine Research, 23* (2022), 11, pp. 1879-1898

[6]Surisetty, V.R., et al., Alcohols As Alternative Fuels: An Overview, *Applied Catalysis A: General, 404* (2011), 1, pp. 1-11

[7]Zhen, X., Wang, Y., An Overview Of Methanol As An Internal Combustion Engine Fuel, *Renewable and Sustainable Energy Reviews*, *52* (2015), pp. 477-493

[8]Ainsalo, A., et al., OPTICAL INVESTIGATION OF SPRAY CHARACTERISTICS FOR LIGHT FUEL OIL, KEROSENE, HEXANE, METHANOL, AND PROPANE, *Atomiz Spr*, *29* (2019), 6, pp. 521-544

[9]Matamis, A., et al., Optical Characterization Of Methanol Compression-Ignition Combustion In A Heavy-Duty Engine, *Proceedings of the Combustion Institute*, *38* (2021), 4, pp. 5509-5517

[10] Badawy, T., et al., Macroscopic Spray Characteristics Of Iso-Octane, Ethanol, Gasoline And Methanol From A Multi-Hole Injector Under Flash Boiling Conditions, *Fuel*, *307* (2022), pp. 121820

[11] Zeng, W., et al., Characterization of Methanol and Ethanol Sprays from Different DI Injectors by Using Mie-scattering and Laser Induced Fluorescence at Potential Engine Cold-start Conditions, *Proceedings*, April 12, 2010, pp. 2010-01-0602

[12] Chen, Z., et al., Effect Of Fuel Temperature On The Methanol Spray And Nozzle Internal Flow, *Applied Thermal Engineering*, *114* (2017), pp. 673-684

[13] Wu, F., et al., Experimental Study Of Methanol Atomization And Spray Explosion Characteristic Under Negative Pressure, *Process Safety and Environmental Protection*, *161* (2022), pp. 162-174

[14] Li, G., et al., Analysis Of Micro-Mixing And Chemical Kinetic Effects Of Ultra-Lean Methane-Air Mixture Ignited By Turbulent Jets, *Fuel*, *341* (2023), pp. 127604

[15] Abramovich, L., et al., CARBURETOR TYPE INTERNAL COMBUSTION ENGINE WITH PRECHAMBER, *Proceedings*, 2017

[16] Long, W., et al., Effects Of Dual-Direct Injection Parameters On Performance Of Fuel Jet Controlled Compression Ignition Mode On A High-Speed Light Duty Engine, *Fuel*, *235* (2019), pp. 658-669

[17] Li, B., et al., Multiple-Objective Optimization Of Jet Controlled Compression Ignition (JCCI) Mode With Dual-Direct Injection In A High-Speed Light-Duty Engine, *Fuel*, *333* (2023), pp. 126327

[18] Tang, Q., et al., Optical Diagnostics On The Pre-Chamber Jet And Main Chamber Ignition In The Active Pre-Chamber Combustion (PCC), *Combustion and Flame*, *228* (2021), pp. 218-235

[19] Tang, Q., et al., Study On The Effects Of Narrow-Throat Pre-Chamber Geometry On The Pre-Chamber Jet Velocity Using Dual Formaldehyde PLIF Imaging, *Combustion and Flame*, *240* (2022), pp. 111987

[20] García-Oliver, J.M., et al., An Experimental And One-Dimensional Modeling Analysis Of Turbulent Gas Ejection In Pre-Chamber Engines, *Fuel*, *299* (2021), pp. 120861

[21] Liu, Z., et al., Enhanced Combustion Of Ammonia Engine Based On Novel Air-Assisted Pre-Chamber Turbulent Jet Ignition, *Energy Conversion and Management*, *276* (2023), pp. 116526

[22] Liu, Z., et al., Experimental Investigation On The Performance Of Pure Ammonia Engine Based On Reactivity Controlled Turbulent Jet Ignition, *Fuel*, *335* (2023), pp. 127116

[23] Liu, Z., et al., Reactivity Controlled Turbulent Jet Ignition (RCTJI) For Ammonia Engine, *International Journal of Hydrogen Energy*, *48* (2023), 33, pp. 12519-12522

[24] Xu, C., et al., Laminar Flame Characteristcs Of Ethanol-Air Mixture: Experimental And Simulation Study, *Therm sci*, *22* (2018), 3, pp. 1453-1444

[25] Oppong, F., et al., An Experimental And Numerical Study Of Propyl Acetate Laminar Combustion Characteristics, *Combustion and Flame, 268* (2024), pp. 113651

[26] Wang, Q., et al., Laminar Burning Velocity And Explosion Characteristics Of A Lignocellulose-Derived Bio-Jet Fuel At Elevated Pressures And Temperatures, *Fuel*, *383* (2025), pp. 133834

Submitted: 25.03.2025
Revised : 20.05.2025
Accepted: 29.05.2025